Molecular Cell, Volume *72*

Supplemental Information

Exon Junction Complex Shapes the Transcriptome by Repressing Recursive Splicing

Lorea Blazquez, Warren Emmett, Rupert Faraway, Jose Mario Bello Pineda, Simon Bajew, Andre Gohr, Nejc Haberman, Christopher R. Sibley, Robert K. Bradley, Manuel Irimia, and Jernej Ule

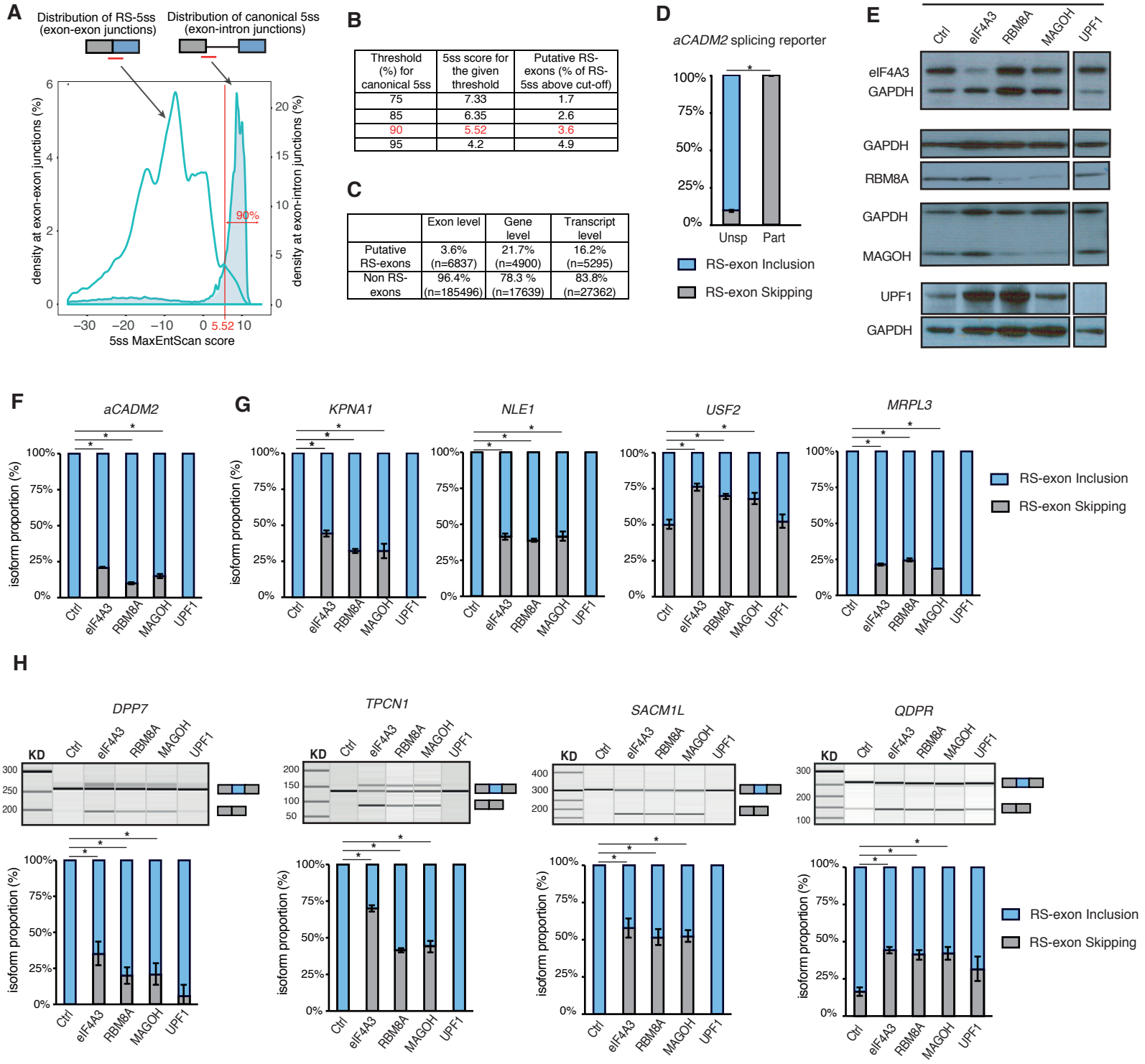

Threshold (%) for canonical 5ss	5ss score for the given threshold	Putative RS-exons (% of RS-5ss above cut-off)
75	7.33	1.7
85	6.35	2.6
90	5.52	3.6
95	4.2	4.9

	Exon level	Gene level	Transcript level
Putative RS-exons	3.6% (n=6837)	21.7% (n=4900)	16.2% (n=5295)
Non RS-exons	96.4% (n=185496)	78.3 % (n=17639)	83.8% (n=27362)

Figure S1. Related to Figure 1: Core EJC components promote inclusion of putative 'RS-exons', which are abundant in the transcriptome
A. Distribution of annotated exons according to their canonical 5ss MaxEntScan score (filled) or their RS-5ss at preceding exon-exon junction (line). The red line denotes the threshold above which 90% of all canonical 5ss are located and the number in red is the 5ss cut-off value associated with that threshold. **B.** Table showing the 5ss MaxEntScan scores associated with different thresholds and the proportion of putative RS-exons according to that 5ss cut-off value. In red, the threshold selected to quantify "putative RS-exons". **C.** Table showing the proportion of RS-exons at exon, gene and transcript level according to ENSEMBL GCRh37 annotation. **D.** Quantification of RT-PCR experiments shown in Figure 1C. **E.** Western-blot validation of eIF4A3, RBM8A, MAGOH and UPF1 protein depletion after siRNA transfection in HeLa cells. GAPDH is used as an input control. UPF1 KD sample was run in the same gel, but it is shown as a separate box as there were other lanes in between that are not shown. **F.** Quantification of RT-PCR experiments shown in Figure 1D. **G.** Quantification of RT-PCR experiments shown in Figure 1G **H.** RT-PCR validation and quantification of RS-exon skipping events in 4 different genes after KD of EJC core factors or UPF1 in HeLa cells (n=3, 3 independent experiments). For figures B, D, E and F, blue and grey columns indicate the percentage of RS-exon inclusion and skipping isoforms respectively. Data are mean ± standard deviation. *P<0.05.

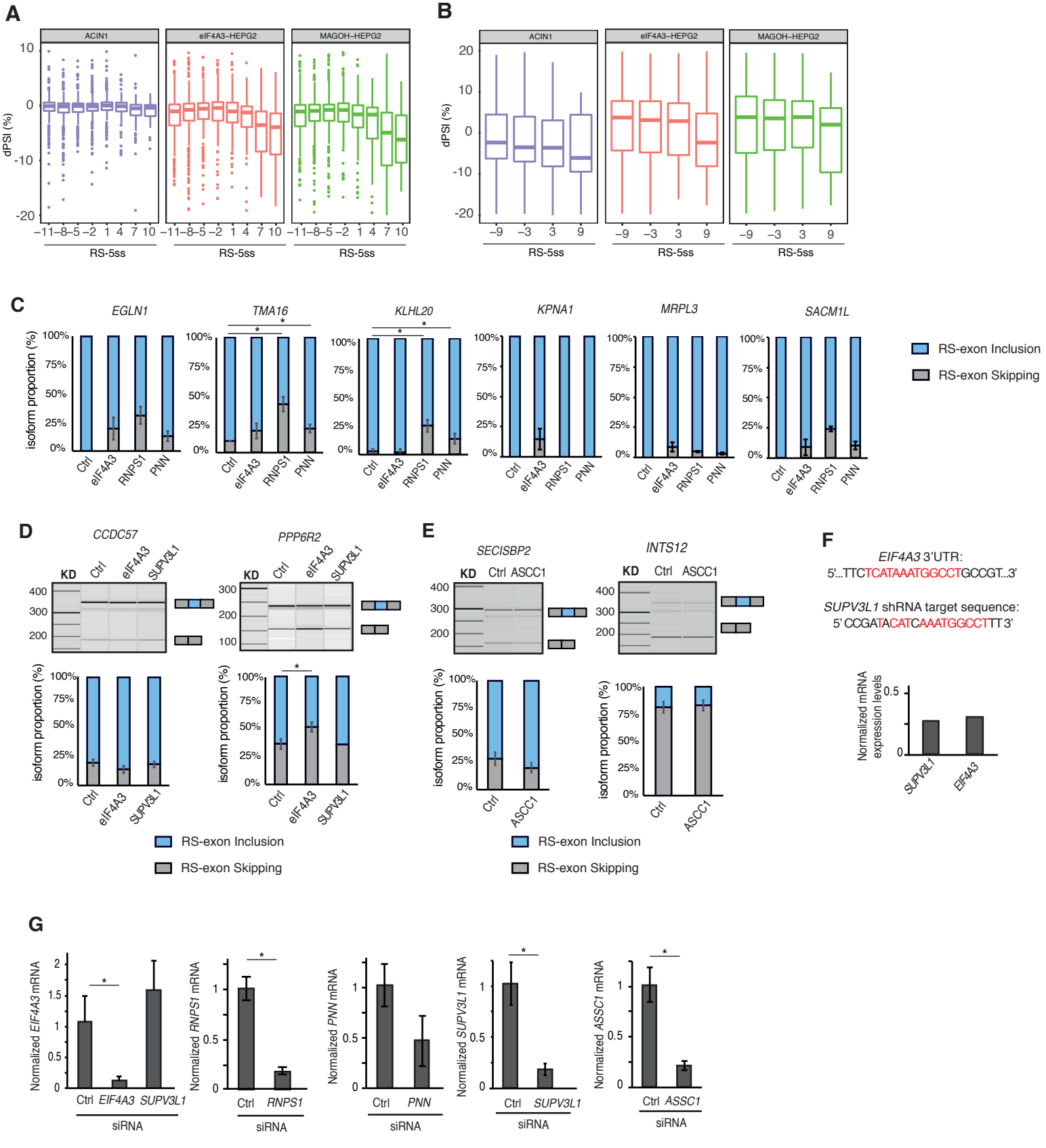

Figure S2. Related to Figure 2: PNN and RNPS1 contribute to the inclusion of 'annotated RS-exons'

A. Box plots representing the difference in percentage spliced in (dPSI) in highly included exons (PSI>90%) after knocking down different RBPs. Exons are binned by their RS-5ss score and dPSI for each bin is calculated by comparing its average PSI in each knockdown experiment to the control experiment.The RS-5ss values in the x-axis indicate the midpoint of each group. Negative dPSI values indicate exon skipping. **B.** Same as A but for alternative exons with PSI < 90%. **C.** Quantification of RT-PCR experiments shown in Figure 2E (n=3, 3 independent experiments, except for *EGLN1, KPNA1, MRPL3* and *SACM1L*, where n=2). **D-E.** RT-PCR Qiaxcel images (top) and quantification (down) of RS-exon skipping events upon *SUPV3L1* (D) or *ASCC1* (E) KD. eIF4A3 KD was included when *SUPV3L1* was knocked-down for comparison (n=3, 3 independent experiments). For quantification of RT-PCR experiments shown in C-E, blue and grey columns indicate RS-exon inclusion and skipping respectively. Data are mean ± standard deviation. *P<0.05. **F.** Diagram indicating *SUPV3L1* shRNA target sequence and *EIF4A3* 3'UTR sequence. The nucleotides shared in both sequences are indicated in red. Below, quantification of *SUPV3L1* and *EIF4A3* mRNA levels in SUPV3L1 KD ENCODE RNA-seq data showing that SUPV3L1 KD leads to a decrease in *EIF4A3* expression level. **G.** Quantification of *EIF4A3*, *RNPS1, PNN*, *SUPV3L1* and *ASCC1* mRNA levels by qPCR after their respective KD using gene-specific siRNAs (n=3, 3 independent experiments).

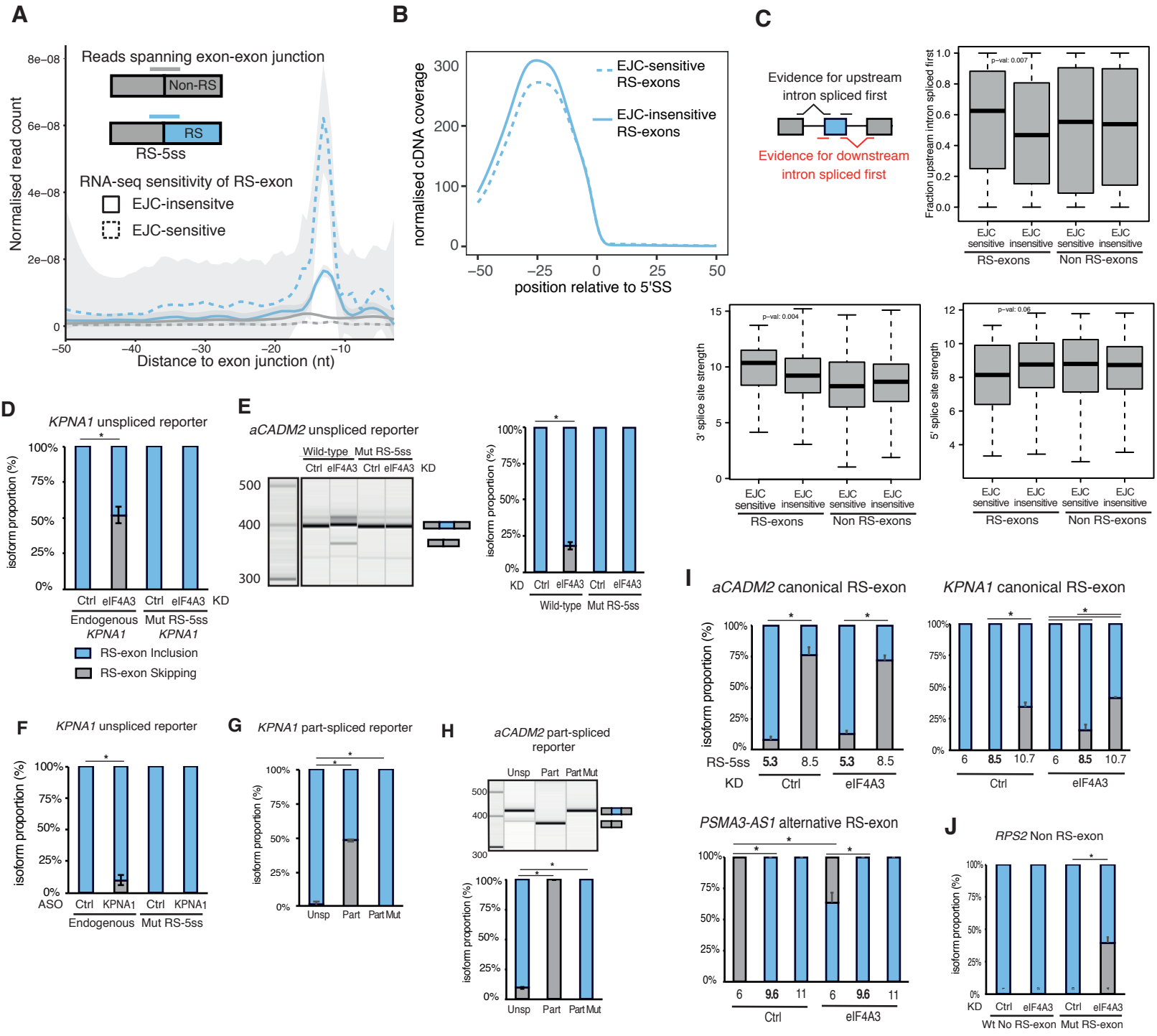

Figure S3. Related to Figure 3: Skipping of annotated RS-exons upon EJC KD results from recursive splicing

A. Metaprofile of the distance between read starts and exon-exon junctions from PRPF8 iCLIP in HeLa cells treated with eIF4A3 siRNA (n=4, 2 independent experiments). Reads that span exon-exon junctions at the 5' end of an RS-exon or non RS-exon are plotted in blue or gray respectively. Read counts have been normalised by the total number of crosslinks for each sample and the total number of exons in each class (RS sensitive = 890, RS insensitive = 3,741, non-RS sensitive = 14,486, non-RS insensitive = 115,924).The data was smoothed using LOESS with a span of 0.2. Shaded regions represent 95% confidence intervals. Exons containing only one read across all 8 samples were excluded from the analysis. **B.** Density plot showing the normalised cDNA coverage of eIF4A3 and BTZ iCLIP crosslinking around the 5ss upstream of RS-exons that are EJC-sensitive (green line, ΔPSI<-0.15 in KD of eIF4A3, RBM8A and/or CASC3) and EJC-insensitive (gray line, remaining RS-exons with >10 junction reads) in HeLa cells. **C**. Top left: Diagram showing the reads from RNAseq data used to analyse intron splicing order. Top right and below: Box plots showing the fraction of reads supporting co-transcriptional splicing and 3ss and 5ss scores in 4 different categories of highly included exons (PSI > 85). RS-exons are classified as having a RS-5ss MaxEntScan score of 5.52 or higher. EJC sensitive exons have a dPSI<-0.1 upon eIF4A3 knockdown whereas EJC insensitive exons are -0.02<dPSI< 0.02. **D.** Quantification of RT-PCR experiments shown in Figure 3C. **E.** Left: Qiaxcel analysis of endogenous or mutant *aCADM2* RS-exon splicing pattern after eIF4A3 KD in HeLa Flp-In cells which stably express wild-type or mutant RS-5SS *aCADM2* splicing reporters (n=3, 3 independent experiments). Right: Quantification of RT-PCR experiments shown in the left. **F.** Quantification of RT-PCR experiments shown in Figure 3D. **G.** Quantification of RT-PCR experiments shown in Figure 3E. **H.** Top: Qiaxcel analysis of *aCADM2* RS-exon splicing pattern after transient transfection of unspliced (Unsp), part-spliced (Part) and part-spliced mutant (Part Mut) plasmids in HeLa cells (n=3, 3 independent experiments). Bottom: Quantification of RT-PCR experiments shown on top. **I.** Quantification of RT-PCR experiments shown in Figure 3F. **J.** Quantification of RT-PCR experiments shown in Figure 3H. For quantification images shown in B to H, blue and grey columns indicate the percentage of RS-exon inclusion and skipping isoforms respectively. Data are mean ± standard deviation. *P<0.05.

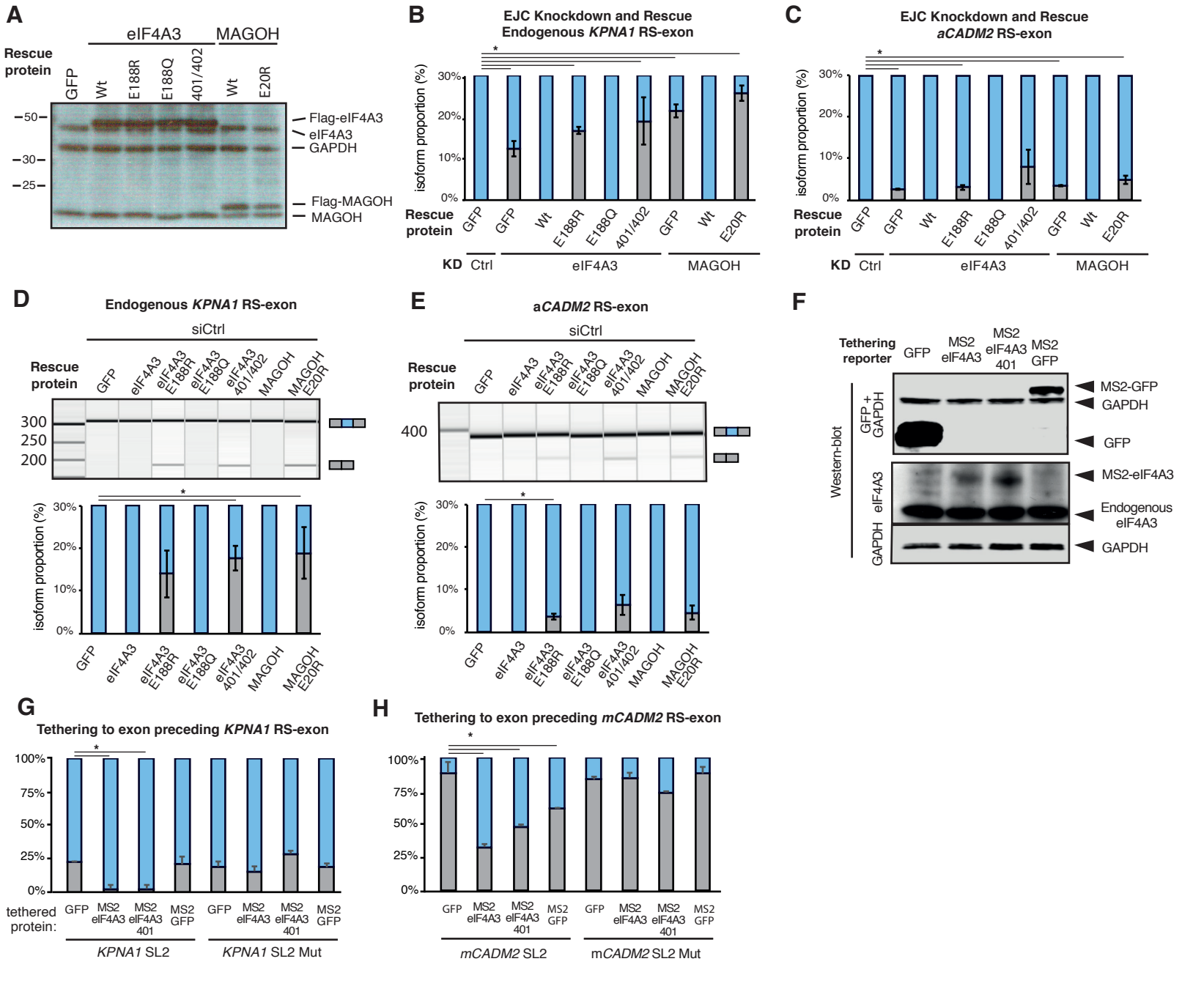

Figure S4. Related to Figure 4: Stable EJC deposition is required to block recursive splicing

A. Western-blot of eIF4A3 and MAGOH proteins to validate the expression of siRNA resistant Flag-tagged EJC components in HeLa cells. GAPDH is used as an input control. **B-C.** Quantification of *KPNA1* (B) and *aCADM2* (C) RS-exon splicing shown in Figure 4A (n=3, 3 independent experiments). **D-E.** Qiaxcel analysis (up) and quantification (down) of *KPNA1* (D) or a*CADM2* (E) RS-exon splicing pattern after overexpression of wild-type or mutant Flag-tagged EJC components in a control siRNA background (n=3, 3 independent experiments). **F.** Western-blot of MS2-rescue proteins used in tethering experiments.GAPDH is used as an input control. **G-H.** Quantification of *KPNA1 (*G) and *mCADM2* (H) RS-exon splicing shown in Figure 4B (n=3, 3 independent experiments). For quantification images shown in B to E and G-H, blue and grey columns indicate RS-exon inclusion and skipping respectively. Data are mean ± standard deviation. *P<0.05.

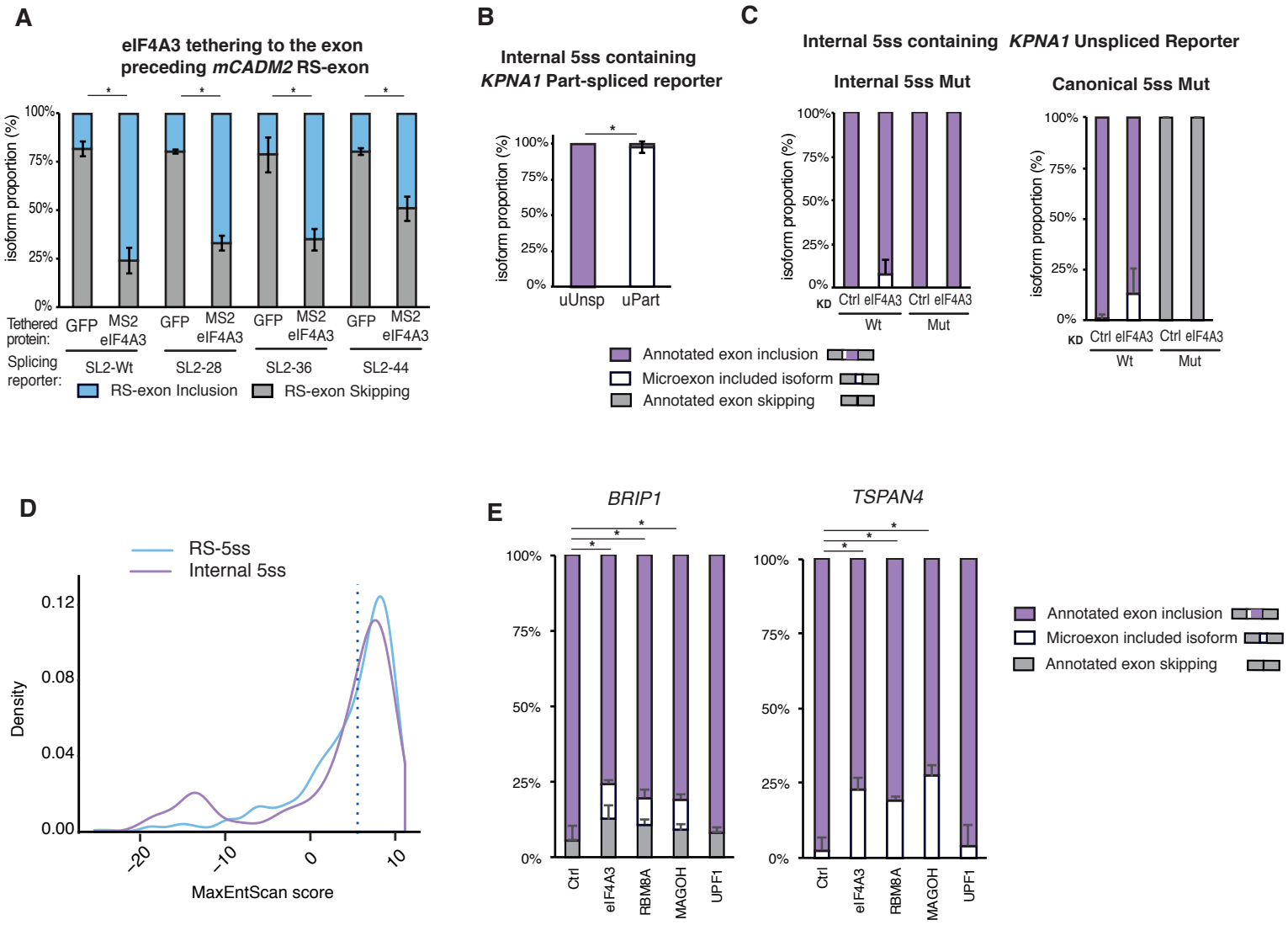

Figure S5. Related to Figure 5: EJC depletion leads to inclusion of cryptic microexons

A Quantification of RT-PCR experiments shown in Figure 5A. Blue and grey columns indicate the percentage of RS-exon inclusion and skipping isoforms respectively. Data are mean ± standard deviation. *P<0.05. **B** Quantification of RT-PCR experiments shown in Figure 5B. Purple and white columns indicate inclusion of annotated exon or microexon containing isoform respectively. Data are mean ± standard deviation. *P<0.05. **C** Quantification of RT-PCR experiments shown in Figure 5C. Purple and white columns indicate inclusion of annotated exon or microexon containing isoform respectively. Data are mean ± standard deviation. *P<0.05. **D** Density plot showing the distribution of RS-5ss MaxEntScan scores for RS-exons and cryptic 5ss MaxEntScan scores for cryptic microexons with dPURS >= 10 in HeLa cells. **E** Quantification of Qiaxcel images shown in Figure 5E. Purple and white columns indicate inclusion of annotated exon or microexon containing isoforms respectively. Grey columns in *BRIP1* represent annotated exon skipping isoform. Data are mean ± standard deviation. *P<0.05.

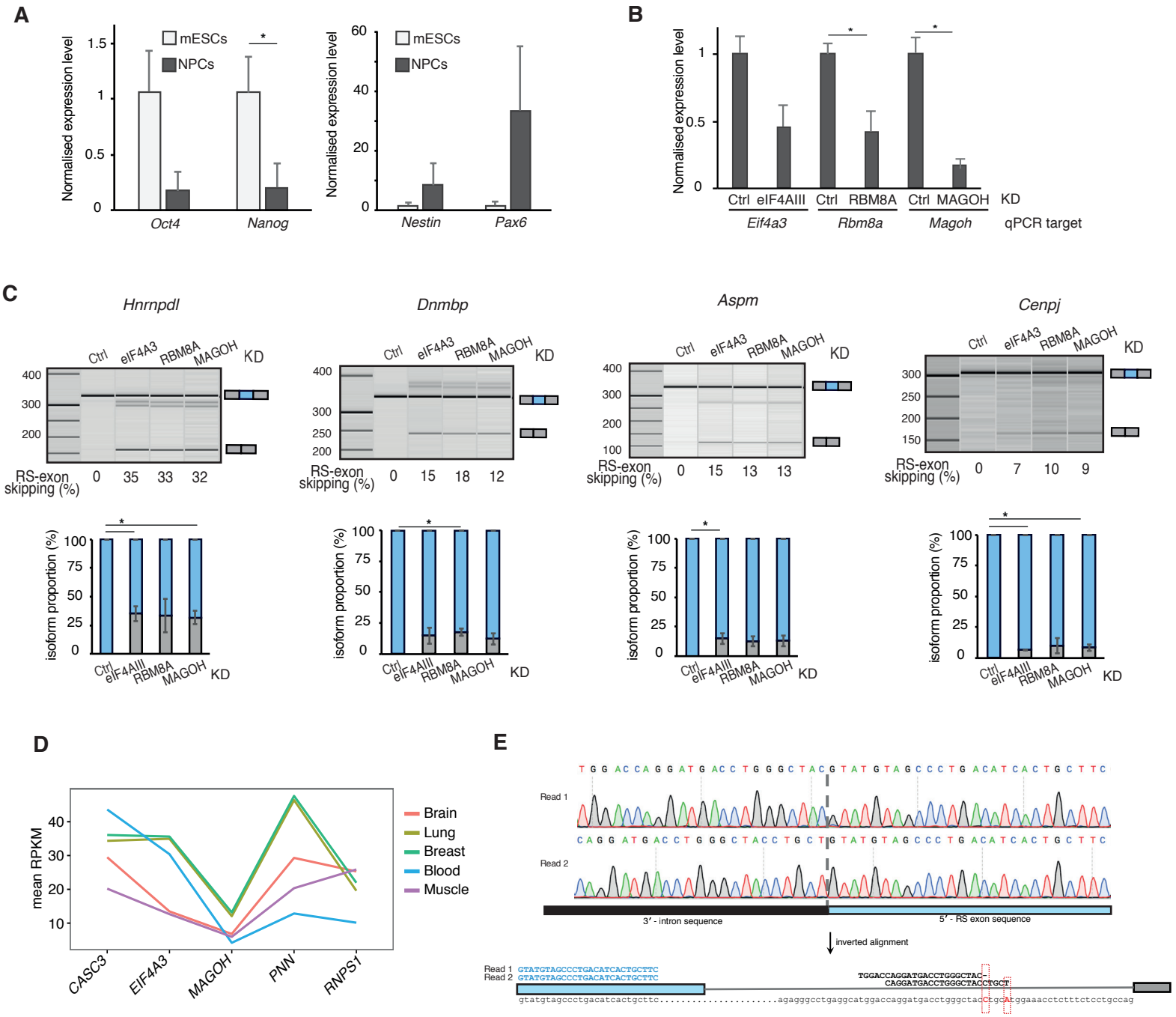

Figure S6. Related to Figure 6: EJC-mediated repression of Recursive splicing in the brain and physiologic alternative splicing of RS-exons
A. Quantification of the expression level of mESC (Oct4 and Nanog) and NPC (Nestin and Pax6) specific genes by qRT-PCR (n=3, 3 independent experiments). Data are mean ± standard deviation. *P<0.05. **B.** Quantification of Eif4a3, Rbm8a and Magoh mRNA levels by qPCR after their respective KD using shRNAs (n=3, 3 independent experiments). Data are mean ± standard deviation. *P<0.05. **C.** Top: Qiaxcel RT-PCR validation of RS-exon skipping events in neuronal precursor cells (NPCs) derived from mouse embryonic stem cells (mESCs) after depletion of core EJC components (n=3, 3 independent experiments). Bottom: Quantification of RT-PCR experiments shown in Figure 6C. Blue and grey columns indicate RS-exon inclusion and skipping respectively. Data are mean ± standard deviation. *P<0.05. **D.** Line graph depicting the mean RPKM of EJC factors across 5 tissues as defined by the GTEx RNA-seq data. **E.** Chromatograms of Sanger-sequencing results showing DNA sequences supporting RS-lariats. Two different sequences supporting the usage of alternative branchpoints were obtained.

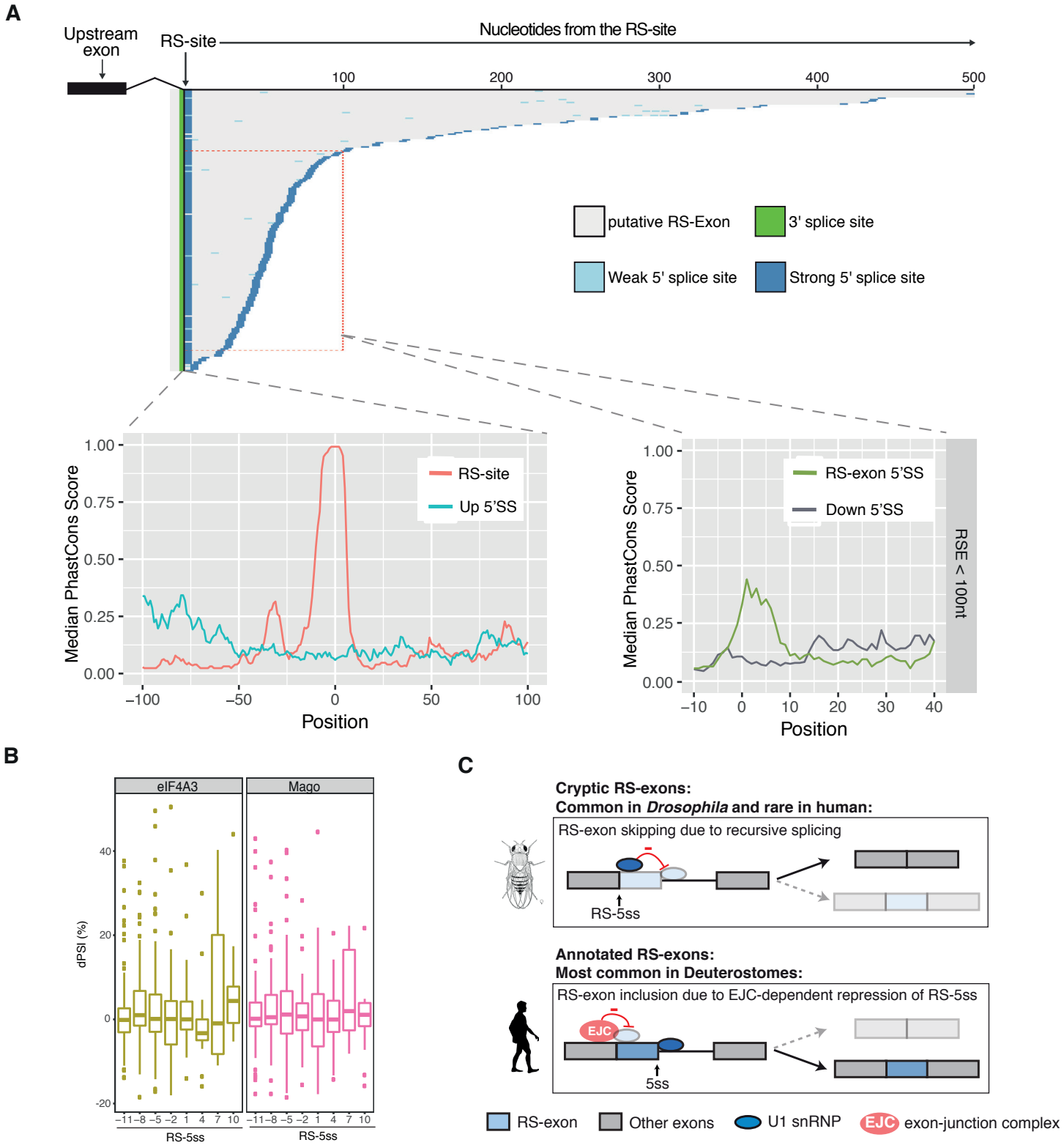

Figure S7: Related to Figure 7: Analysis of RS-exons inclusion across evolution

A. Top: Graphical representation of the RS-sites previously annotated in *D. melanogaster* and the nearest 5ss present downstream of them. The sequence between both sites is considered a putative RS-exon. Bottom: Sequence conservation analysis of the region downstream the RS-sites that contain a strong 5ss sequence within a 100nt window. Conservation strength is shown in red for RS-sites, blue for the nearest upstream 5ss (Up 5ss), green for the nearest downstream 5ss (RS-exon 5ss) and grey for further downstream 5ss (Down 5ss). **B.** Box plots representing the difference in percentage-spliced-in (dPSI) of exons after knocking down eIF4A3 or Mago in Drosophila S2 cells. Exons are binned by their RS-5ss score and dPSI for each bin is calculated by comparing its average PSI in each knockdown experiment to the control experiment.The RS-5ss values in the x-axis indicate the midpoint of each group. Negative dPSI values indicate exon skipping. **C.** RS-exon skipping due to recursive splicing, which leads to cryptic RS-exons, appears to be common in *Drosophila* but rare in human, whereas the proportion of canonical RS-exons is increased in Deuterostomes.

Table S1: Target site sequences of siRNAs, Related to STAR Methods	
Gene name	**Sequence**
MAGOH	CGGGAAGUUAAGAUAUGCCA
MAGOHB	CAGGCUGUUUGUAUAUUUAAU
EIF4A3-3UTR	GCAGCAGATCAGTGGGATGAG
MAGOH-3UTR	CTGAATATTGGTGTGGACA
SUPV3L1	CCGATACATCAAATGGCCTTT
ASCC1	GAATCATTTGATGGCCGAAAT
RNPS1	GCATCCAGCCGCTCAGGAA
PNN	GGTAAGGTGGCTCAGCGAG
RBM8A	CGCTCTGTTGAAGGCTGGA
CASC3	GATCGGAAGAATCCAGCAT

Table S2: Oligonucleotides sequences used for cloning, Related to STAR Methods	
Name	**Sequence**
PSMA3 Fw-I	ACTCGAAAGCTTAGCTTGTCGGCGCCATTTTG
PSMA3 Rv-I	ATCGATTGGATCCGGTTACGAAGTTTACCATGGCTGCCTG
PSMA3 Fw-II	CGTAACCGGATCCAATCGATATCGCAGTCTTTAAGTTACA
PSMA3 Rv-II	ATCGATTGAATTCGGTTACGGTCTTATCAGGCTACAAAAG
PSMA3 Fw-III	CGTAACCGAATTCAATCGATAGCAAATTTGTGTGTGTGGT
PSMA3 Rv-III	ACTCGAGCGGCCGCCACAAACAGATCGCAGATCC
PSMA3_6_Fw	TGTGTAGCAAAATGTTTCACTGTACAAATTCCCACCTAAAGTGAAAAAAAAAAAAAAGTG
PSMA3_6_Rv	CACTTTTTTTTTTTTTTTCACTTTAGGTGGGAATTTGTACAGTGAAACATTTTGCTACACA
PSMA3_11_Fw	CCACTTTTTTTTTTTTTTTCACTTTAGGTAAGTATTTGTACAGTGAAACATTTTGCTACACA
PSMA3_11_Rv	TGTGTAGCAAAATGTTTCACTGTACAAATACTTACCTAAAGTGAAAAAAAAAAAAAAGTGG
aCADM2_8.5_Fw	CTGATTACACTGGAATGATTAATGTACTTACCTAAAACAGAAAGAAATAAAACA
aCADM2_8.5_Rv	TGTTTTATTTCTTTCTGTTTTAGGTAAGTACATTAATCATTCCAGTGTAATCAG
KPNA1_6_Fw	ACTCTGCAGAGCTGAGCAATTCAGCATCACCTAAAAGAAAAAGTTTGAAAAT
KPNA1_6_Rv	ATTTTCAAACTTTTTCTTTTAGGTGATGCTGAATTGCTCAGCTCTGCAGAGT
KPNA1_10.7_Fw	TAAAATTTTCAAACTTTTTCTTTTAGGTAAGACTGAATTGCTCAGCTCTGCAGAG
KPNA1_10.7_Rv	CTCTGCAGAGCTGAGCAATTCAGTCTTACCTAAAAGAAAAAGTTTGAAAATTTTA
HindIII_MainCADM2_1444Fw	ACTCGAAAGCTTCTGCTGCCGCCGATCCGAGT
CADM2_Main_SL2_Rv	GGCACGGCTGATGCTCGTGCTTTGGAGAACGGCGCTGCGTTTC
CADM2_Main_SL2-Int_Fw	AGCACGAGCATCAGCCGTGCCTCGCTACAAGGTAATCCCCGCC
p5_2364NotI_Rv	ACTCGAGCGGCCGCCAGTGTGATGGATATCTGCA
KPNA1 MS2-Mut_Fw	GGCACGGCTCATGCTCGTGCTTTTCCC
KPNA1 MS2-Mut_Rv	GGGAAAAGCACGAGCATGAGCCGTGCC
CADM2_SL2Mut_Fw	GGCACGGCTCATGCTCGTGCTTTGGAG
CADM2_SL2Mut_Rv	CTCCAAAGCACGAGCATGAGCCGTGCC
E188Q Fw	ACGTGCTATCAAAATGTTGGTTTTGGATCAAGCTGATGAAATGT
E188Q Rv	ACATTTCATCAGCTTGATCCAAAACCAACATTTTGATAGCACGT
GFP_Fw_XhoI	ACTCGACTCGAGATGGTGAGCAAGGGCGAGGA

GFP_Rv_NotI	ACTCGAGCGGCCGCTCACTTGTACAGCTCGTCCATGC
mMagoh shRNA Fw	CCGGGCAAGTTCGGTCATGAGTTCCAATCTCGAGATTGGAACTCATGACCGAACTTGCTTTTTG
mMagoh shRNA Rv	AATTCAAAAAGCAAGTTCGGTCATGAGTTCCAATCTCGAGATTGGAACTCATGACCGAACTTGC
mRbm8a shRNA Fw	CCGGGCGGACCTTGTGTTTATATTTAATCTCGAGATTAAATATAAACACAAGGTCCGCTTTTTG
mRbm8a shRNA Rv	AATTCAAAAAGCGGACCTTGTGTTTATATTTAATCTCGAGATTAAATATAAACACAAGGTCCGC
meIf4a3 shRNA Fw	CCGGGAGGAGGACATGACCAAAGAATCTCGAGATTCTTTGGTCATGTCCTCCTCTTTTTG
meIf4a3 shRNA Rv	AATTCAAAAAGAGGAGGACATGACCAAAGAATCTCGAGATTCTTTGGTCATGTCCTCCTC
mControl shRNA Fw	CCGGCGGCTGAAACAAGAGTTGGAATCTCGAGATTCCAACTCTTGTTTCAGCCGTTTTTG
mControl shRNA Rv	AATTCAAAAACGGCTGAAACAAGAGTTGGAATCTCGAGATTCCAACTCTTGTTTCAGCCG

Table S3: Oligonucleotides sequences used for PCR/RT-PCR, Related to STAR Methods	
Name	**Sequence**
KPNA1 Exon 10 Fw	AGTGGTTTCTCCTGCTTTGC
KPNA1 Exon 12 Rv	GCTGATCCTCCAGAAGTTGC
KPNA1 Exon13 Rv	CAGAGCGGCTTGATACAACC
BGHpA Rv	TTAGGAAAGGACAGTGGGAG
aCADM2 Fw	GCTGTCACCTCTCAATATCACAAG
mCADM2 Fw	TTCCTTCCCCAGCCCTTTAG
USF2 Fw	GCGACCACAACATCCAGTAC
USF2 Rv	ACACTGGACGCTGGGAAATA
DPP7 Fw	TGTCAGACGAGAAGGACCTG
DPP7 Rv	GTAGAGCCGGTAGATGTCGT
NLE1 Fw	ACTGAAGGTGTGGGATGTGA
NLE1 Rv	CAGCCTTTGTTCTCTGGCAG
MRPL3 Fw	CCAAGGATGGTCAAAAGCAT
MRPL3 Rv	GCCTGGTTTAATTGCAGCT
TPCN1 Fw	TTTGATGAGCTTCCCAGGAC
TPCN1 Rv	GTCTCCACGAGGATCCAGAC
SACM1L Fw	TCCTCCTTCAGCTGTCACAA
SACM1L Rv	CGCTGCAAAGTATGGGTCAA
QDPR Fw	ATCGACCATCTCCAGCCATC
QDPR Rv	GCATTGATTTCCTGTTCATCGG
TMA16_Fw	TCAAAGAAAGATGCTTGTGAACT
TMA16_Rv	TTTCCTCTTGCACGTCTTGG
KLHL20_Fw	GTTGGTGCAGTGGAGATGC
KLHL20_Rv	AGAACCCTCCTAACACAGCC
RAD7_Fw	TATAGAGGAAAGGGGCCAAGA
RAD7_Rv	GGTTGCCTTTCTAAAACTTGAGC
EMG1_Fw	CAGTGTTCGAGCAGCTGATG
EMG1_Rv	AAGTTTTGCACAGGTGAGGG
CCDC57_Fw	TGCCTGGGATGCTCAAATTG
CCDC57_Rv	CCACCTCCTGCTCCTGTAG
GANC_Fw	CAGCACCAGGTTCCAAATCA
GANC_Rv	CCTGTTCCTGGCCATTTCTG
PPR6R2_Fw	GAGAGCTTCGTGGAGGAGAC
PPR6R2_Rv	TGATGTTGTCGTCCTGGTCG
SECISBP2L_Fw	TTGGTCCAATGTAACTTGC
SECISBP2L_Rv	TCTCATCCTTAGCATTTCCA
INTS12_Fw	CGGGAACAGACGGATCGG

INTS12_Rv	AACTGGAATCAATGCCCCGA
mHnrnpdl_Fw	GCAACAACAGAAAGGAGGCA
mHnrnpdl_Fw	CCCAGCGTCCTCCTTTAGTA
mAspm_Fw	CCCTTGGGTTGCTTTGGAAA
mAspm_Rv	ACGGGTGGTAATGGTGGATC
mDnmbp_Fw	TGGAGAAGAGAGCCAAGGTG
mDnmbp_Fw	AGGTGCTTCTGGGTCTTCTC
mFlna_Fw	TGGGACTCCTGGGATGCTA
mFlna_Fw	CTTCTCCCTGTCCAGCACTT
RPS2_Fw	GATTATGCCAGTGCAGAAGC
TSPAN4_Fw	TCCTCTTCTTCGCCTACACG
TSPAN4_Rv	AAGCAGCAGGAGTCAGGTAC
HSPD1_Fw	CAGTCCATTGTACCTGCTCTTG
HSPD1_Rv	AAGTCATGAGGCTGAACGTC
BRIP1_Fw	ACACAGAAATGATTGGGGAGC
BRIP1_Rv	TTGTTTGTTGAAAGTTGGGCT
RPL18A_Fw	GACACTTCCTTTTGCGGGTG
RPL18A_Rv	ATTCCCGGTACATGTTGTGG
AP1G2-RS-outer_Fw	AGGGGACTAAGGGGGACAG
AP1G2-RS-outer_Rv	CTGAGGGAGGCATCAGTTTC
AP1G2-RS-inner_Fw	GACAGGTCCCTGGGGAAG
AP1G2-RS-inner_Rv	CTGAGGGAGGCATCAGTTTC
AP1G2-Std-outer_Fw	GCAGTGATAGAGGGGACAGG
AP1G2-Std-outer_Rv	TCAGACTGCACCAGTCGAAG
AP1G2-Std-inner_Fw	GCAGTGATAGAGGGGACAGG
AP1G2-Std-inner_Rv	CAGGAGGCTCTGGAGGAAG
AP1G2-upstream of RSE-outer_Fw	TCCCTATACCCAGGACAGGAC
AP1G2-upstream of RSE-outer_Rv	CAGGAGGCTCTGGAGGAAG
AP1G2-upstream of RSE-inner_Fw	TCCCTATACCCAGGACAGGAC
AP1G2-upstream of RSE-inner_Rv	GAGGCTCTGGAGGAAGGAG
AP1G2-downstream of RSE-outer_Fw	GACAGGTCCCTGGGGAAG
AP1G2-downstream of RSE-outer_Rv	TAAACTGGCTCGAGTCTTGG
AP1G2-downstream of RSE-inner_Fw	ACCAGGATGACCTGGGCTAC
AP1G2-downstream of RSE-inner_Rv	TAAACTGGCTCGAGTCTTGG
mago_dsRNA_Fw	taatacgactcactatagggCCGTGTGTTTTCCCATCTCT
mago_dsRNA_Rv	taatacgactcactatagggGCCCTCGGGATCTTTTGAC
eIF4AIII_dsRNA_Fw	taatacgactcactatagggCCACCTTCTCCATCTCCATC
eIF4AIII_dsRNA_Rv	taatacgactcactatagggGCGACGAAGAACTGCTTGAT

Table S4: Oligonucleotides sequences used for qPCR, Related to STAR Methods	
Name	**Sequence**
EIF4A3_qPCR_Fw	ATGGCGACCACGGCCACGAT
EIF4A3_qPCR_Rv	GTGTCGAACGTGGGGGTCAC
RNPS1_qPCR_Fw	GGACAAAACCCGAAAGAGGC
RNPS1_qPCR_Rv	CCTCCTGTTGTCGTGTCTGC
PNN_qPCR_Fw	ACAAGAATCCACTGTTGCTACTG
PNN_qPCR_Rv	CAAAAGCCGCAGTTCTGTCT
SUPV3L1_qPCR_Fw	TGCAGTCTCATTCCCTGGAT
SUPV3L1_qPCR_Rv	ATTATCTTCCGCTGCATGGC
ASCC1_qPCR_Fw	GAAGTGGAGATGGCAGGGAT
ASCC1_qPCR_Rv	GAAAACGTTCCAGCACTCGA
GAPDH_qPCR_Fw	AAGGTGAAGGTCGGAGTCAA
GAPDH_qPCR_Rv	AATGAAGGGGTCATTGATGG
mEif4a3_Fw	TTTCACTGTGTCGTCCATGC
mEif4a3_Rv	TGTTGGGCAGGTCGTAGTTA
mRbm8a_Fw	GTCACTGGAGTCCACGAAGA
mRbm8a_Rv	GGTCCACGAACAAAACACCA
mMagoh_Fw	ACAAAGGCAAGTTCGGTCAT
mMagoh_Rv	GGCCACAGAGCATCATCTTC
mOct4_Fw	CTTCACCACACTCTACTC
mOct4_Rv	CCAGGTTCTCTTGTCTAC
mNanog_Fw	TGAGCTATAAGCAGGTTAAGAC
mNanog_Rv	CAATGGATGCTGGGATACTC
mNestin_Fw	GTCTCAGGACAGTGCTGAGCCTTC
mNestin_Rv	TCCCCTGAGGACCAGGAGTCTC
mPax6_Fw	GCGGAGTTATGATACCTACACC
mPax6_Rv	GAAATGAGTCCTGTTGAAGTGG
mGAPDH_Fw	AAGGGCTCATGACCACAGTC
mGAPDH_Rv	GGATGACCTTGCCCACAG